

# Enhanced Analytical Performance of Paper Microfluidic Devices by Using Fe<sub>3</sub>O<sub>4</sub> Nanoparticles, MWCNT, and Graphene Oxide

Federico Figueredo,<sup>†,‡</sup> Paulo T. Garcia,<sup>†</sup> Eduardo Cortón,<sup>‡</sup> and Wendell K. T. Coltro<sup>\*,†</sup>

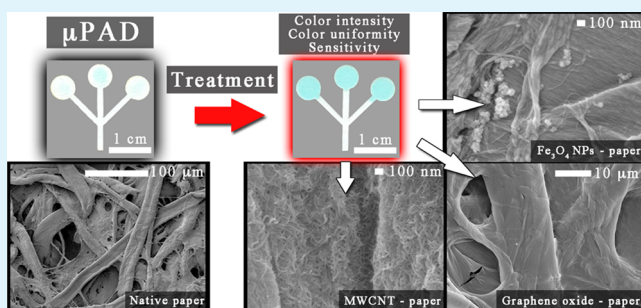
<sup>†</sup>Instituto de Química, Universidade Federal de Goiás, Goiânia, GO 74690-900, Brazil

<sup>‡</sup>Laboratorio de Biosensores y Bioanálisis (LABB), Departamento de Química Biológica e IQUIBICEN–CONICET, Facultad de Ciencias Exactas y Naturales, Universidad de Buenos Aires (UBA), Pabellón 2, Ciudad Universitaria, Ciudad Autónoma de Buenos Aires, Argentina

**S** Supporting Information

**ABSTRACT:** Spheres, tubes, and planar-shaped nanomaterials as Fe<sub>3</sub>O<sub>4</sub> nanoparticles (MNPs), multiwalled carbon nanotubes (MWCNT), and graphene oxide (GO) were used for the first time to treat microfluidic paper-based analytical devices ( $\mu$ PADs) and create a biocompatible layer with high catalytic surface. Once glucose measurements are critical for diabetes or glycosuria detection and monitoring, the analytical performance of the proposed devices was studied by using bienzymatic colorimetric detection of this carbohydrate. The limit of detection values achieved for glucose with  $\mu$ PADs treated with MNPs, MWCNT, and GO were 43, 62, and 18  $\mu$ M, respectively. The paper surface modification solves problems associated with the lack of homogeneity on color measurements that compromise the sensitivity and detectability levels in clinical diagnosis.

**KEYWORDS:** carbon nanotubes, cellulose, clinical diagnostics, colorimetric biosensors, digital image analysis, magnetic nanoparticles, paper microfluidics



In the last years, nanomaterials have gained considerable attention because of their high surface and unique mechanical, electrical, optical, and magnetic properties. Several interfaces between different kind of nanomaterials with well-known properties (e.g., composition, shape, size) and biomolecules (e.g., enzymes, DNA, antibodies) have been used for bioassays and biosensing applications, molecular biology and molecular medicine.<sup>1–4</sup> On the other hand, cellulosic substrate is globally recognized as one of the most used tools in chemistry and it was recently rediscovered for the development of microfluidic paper-based analytical devices ( $\mu$ PADs).<sup>5</sup> Paper microfluidic devices have emerged as a new class of disposable microfluidic systems with the capability to be used at point-of-care (POC) applications.<sup>6</sup> In addition, cellulose fiber treatment and further modifications with Ag nanoparticles<sup>6,7</sup> (NPs), ceria NPs,<sup>8</sup> Au NPs,<sup>6,9–12</sup> curcumin NPs,<sup>13</sup> and SiO<sub>2</sub> NPs<sup>14</sup> for analytical applications have been reported in the literature in order to improve the analytical performance and minimize washing effects often observed in lateral flow assays associated with colorimetric detection.<sup>14</sup> However, the study of analytical applications of Fe<sub>3</sub>O<sub>4</sub> magnetic NPs (MNPs), multiwalled carbon nanotubes (MWCNT) and graphene oxide (GO) to modify  $\mu$ PADs, based on colorimetric measurements, has not been reported. MWCNT and GO can increase the linkage of aromatic molecules through  $\pi$ – $\pi$  stacking or van der Waals forces.<sup>15</sup> Furthermore, biomolecules

can be adsorbed into the surface of oxidized carbon-based nanomaterials by electrostatic interaction<sup>1,16–18</sup> or hydrogen bonding.<sup>19</sup> On the other hand, some studies reported reversible noncovalent interaction between MNPs and biomolecules.<sup>20,21</sup> Moreover, a peroxidase mimetic activity of MNPs with a Michaelis–Menten kinetics was found to have high affinity for TMB in comparison to HRP.<sup>22,23</sup> With this background, we describe for the first time a treatment procedure of  $\mu$ PADs by using spheres, tubes and planar shaped nanomaterials as MNPs, MWCNT, and GO. These nanomaterials differ from each other on their surface-to-volume ratio and shape. Moreover, we propose that they can act as support for GOx and HRP immobilization. If the kinetics of the reaction is governed by diffusion, sphere-shaped nanomaterial among others<sup>24</sup> could achieve higher sensitivities. The hypothesis of this study is that the used nanomaterials will enhance the analytical signal for glucose colorimetric detection by improving the available superficial area of the  $\mu$ PADs.

MNPs were synthesized by the co-precipitation method.<sup>25</sup> Hydrodynamic diameter of 35 nm was determined by dynamic light scattering (DLS) (Figure S1). Fourier transform infrared spectroscopy (FT-IR) analysis of particles showed the

**Received:** October 20, 2015

**Accepted:** December 22, 2015

73 characteristic Fe–O bond of  $\text{Fe}_3\text{O}_4$  at  $590\text{ cm}^{-1}$  (Figure S2).  
 74 MWCNT (Sigma–Aldrich,  $\geq 98\%$ , O.D  $\times$  I.D.  $\times$  L  $10\text{ nm} \pm 1$   
 75  $\text{nm} \times 4.5\text{ nm} \pm 0.5\text{ nm} \times 3\text{--}6\text{ }\mu\text{m}$ ) were oxidized by acid  
 76 treatment to improve dispersion in water. GO (Sigma–  
 77 Aldrich) was prepared from a  $2\text{ mg mL}^{-1}$  stock suspension in  
 78 water. Nanomaterials were dispersed in ultrapure water and  
 79 vigorously stirred prior to use.  $\mu\text{PADs}$  were fabricated by  $\text{CO}_2$   
 80 laser using  $20 \times 20\text{ cm}$  filter paper Whatman #1. Additional  
 81 information about the fabrication of  $\mu\text{PADs}$  is available in  
 82 Supporting Information. Paper chips were soaked in a colloidal  
 83 and stable MNPs, MWCNT and GO nanomaterial solution  
 84 during 30 s to obtain MNP- $\mu\text{PADs}$ , MWCNT- $\mu\text{PADs}$ , and  
 85 GO- $\mu\text{PADs}$ , respectively. The  $\mu\text{PADs}$  were dried over a  
 86 hydrophobic plastic film at room temperature for 40 min and  
 87 then laminated on one side with a poly(methyl methacrylate)-  
 88 coated thermosensitive polyester film at  $130\text{ }^\circ\text{C}$ . After the  
 89 manufacturing process, reagents for glucose colorimetric assay  
 90 were spotted in the detection zones. Briefly,  $1\text{ }\mu\text{L}$  of  
 91 chromogenic substrate ( $15\text{ mM TMB}$ ) and enzymatic solutions  
 92 (GOx:HRP,  $120:30\text{ U mL}^{-1}$ ) were added to the detection  
 93 zones in two independent steps and dried for 20 min at room  
 94 temperature. In all cases,  $10\text{ }\mu\text{L}$  of sample solutions were  
 95 disposed at the bottom region of the  $\mu\text{PAD}$  main channel. After  
 96 20 min at  $25\text{ }^\circ\text{C}$ , the devices were digitalized with a desktop  
 97 scanner and analyzed using the arithmetic mean of the pixel  
 98 intensity within each detection zone through Corel Photo–  
 99 Paint graphical software. The fabrication process of  $\mu\text{PADs}$  and  
 100 signal analysis procedure is detailed in Figure 1.

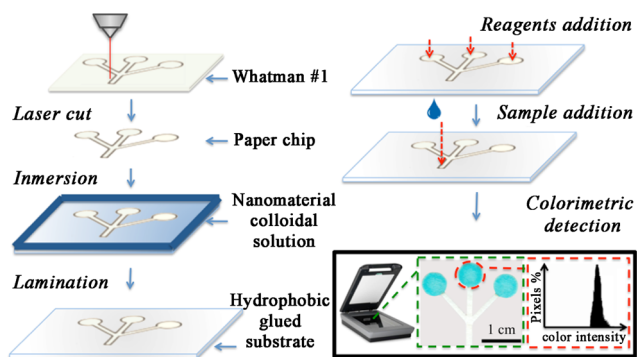


Figure 1. Schematic representation of the construction procedure of the  $\mu\text{PADs}$  showing the treatment step with MNPs, MWCNT, and GO as well as the procedure required for colorimetric detection involving scanner and pixel intensity analysis.

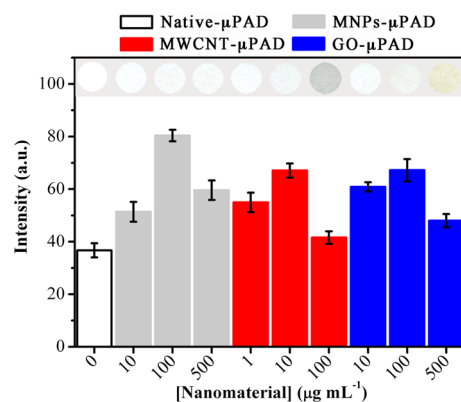


Figure 2. Color intensity of native and treated  $\mu\text{PADs}$  with different concentrations of MNPs, MWCNT, and GO colloidal solutions. Color intensity corresponds to the glucose assay at concentration of  $1\text{ mM}$ . The inset optical micrographs show the background color developed in the paper according to the proposed treatment. Error bars indicate the standard deviation value ( $n = 6$ ).

Additionally, only for higher concentrations of GO ( $1000\text{ }\mu\text{g mL}^{-1}$ ) the  $\mu\text{PAD}$  becomes hydrophobic and therefore lateral flow velocity decreases (data not shown). On the other hand, the low signal response of  $\mu\text{PADs}$  treated with  $500\text{ }\mu\text{g mL}^{-1}$  of MNPs could be due to nanoparticles aggregation (high magnetic forces) over the paper fibers, resulting in a decrease in surface area to volume ratio of the nanoparticles.

To evaluate the peroxidase mimetic behavior of MNPs in the conditions of the bioassay, we performed an additional experiment using MNP- $\mu\text{PADs}$  prepared without HRP. Results indicated that color development was not evident after 20 min of incubation (data not shown) suggesting that the peroxidase activity is not related to MNPs. Figure 3A shows the improvement of the color intensity and uniformity for images captured on detection zones using devices treated with nanomaterial colloidal solutions after glucose addition. It is important to remark that a noticeable difference in color intensity between treated and nontreated  $\mu\text{PADs}$  was found for

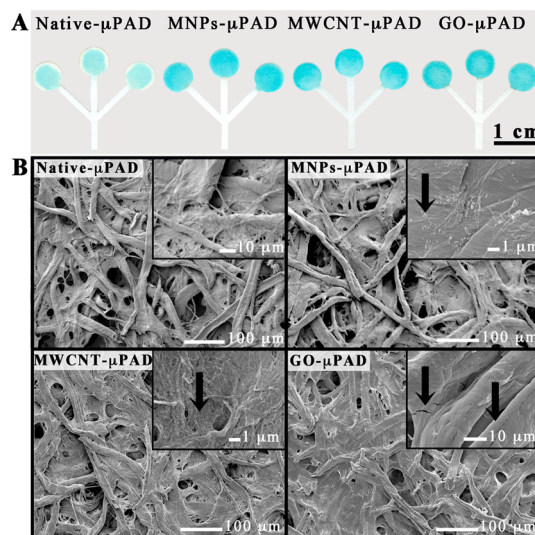


Figure 3. (A) Optical micrograph of  $\mu\text{PADs}$  after addition of  $1\text{ mM}$  glucose sample and (B) FESEM images of native and treated devices with MNPs, MWCNT, and GO. Arrows indicate the presence of nanomaterials over the paper fibers.

135 all treatments. Representative field emission scanning electron  
 136 microscopy (FESEM) images of  $\mu$ PADs used in this study  
 137 (Figure 3B) reveal the presence of the nanomaterials over the  
 138 paper fibers after the treatment procedure. MNPs were  
 139 confirmed by the presence of Fe detected with energy-  
 140 dispersive X-ray spectroscopy (EDS) (Figure S3). The MNPs  
 141 were not evenly distributed over the cellulose material;  
 142 however, when higher concentrations were used (Figure 2),  
 143 low analytical signal was obtained suggesting more aggregation  
 144 and less distribution over the fiber surfaces. The characteristic  
 145 tubular morphology of MWCNT is also shown in Figure 3B.  
 146 GO was detected over the surface of paper due to the presence  
 147 of thin and long edges present on the fibers. In this study,  
 148 diluted nanomaterial colloidal solutions were used to modify  
 149 paper cellulose fibers suggesting physical absorption between  
 150 both materials involving surface forces as hydrogen bonding,  
 151 electrostatic interactions, and van der Waals forces among  
 152 others.<sup>26,27</sup>

153 On the basis of the presented results, the analytical  
 154 performance of the  $\mu$ PADs treated with MNPs, MWCNT  
 155 and GO colloidal solutions were investigated using the  
 156 optimized conditions. For this purpose, analytical curves for  
 157 glucose concentrations ranging from 0 to 5 mM (Figure 4A)  
 158 were obtained and they are displayed in Figure 4. It was  
 159 possible to see that the intensity of the colorimetric signal was  
 160 enhanced in all concentrations of tested glucose. In addition, a

linear relationship for low concentrations of analyte was 161  
 observed using  $\mu$ PADs treated with nanomaterials (Figure 162  
 4B–D). For native  $\mu$ PADs, the colorimetric response offered 163  
 linear behavior from 0.3 to 1 mM (Figure S4) with a limit of 164  
 detection (LOD) of 238  $\mu$ M. Meanwhile for MNP- $\mu$ PAD and 165  
 MWCNT- $\mu$ PAD, the linear range was between 0.05 and 1 mM 166  
 with a LOD of 43 and 62  $\mu$ M, respectively. GO- $\mu$ PAD 167  
 presented the best results with a linear range between 0 and 1 168  
 mM and LOD of 18  $\mu$ M (Table S1). It has been proposed that 169  
 the kinetics of the reaction could be controlled by diffusion 170  
 mechanisms.<sup>24</sup> Higher sensitivities of the analytical method 171  
 could be achieved with MNP- $\mu$ PAD followed by MWCNT- 172  
 $\mu$ PAD and GO- $\mu$ PAD, as was experimentally demonstrated in 173  
 the current study (Table S1). 174

According to optical micrographs presented in Figure 4E, it 175  
 can be seen the visual detection associated with the linear 176  
 increment on the characteristic blue color of TMB in the 177  
 detection zones corresponding to all tested glucose concentra- 178  
 tions. Furthermore, in all cases there is better color intensity 179  
 and uniformity than in native  $\mu$ PADs. LOD values of paper 180  
 devices treated with nanomaterials were lower than native 181  
 $\mu$ PADs and other  $\mu$ PADs recently reported in the literature 182  
 (see Tables S1 and S2). In addition, the use of  $\mu$ PADs treated 183  
 with carbon-based nanomaterials and magnetic nanoparticles 184  
 provided linear response in a glucose concentration range from 185  
 0.05 to 1 mM (MNPs and MWCNT) and from 0 to 1 mM 186  
 (GO), meanwhile for clinical glucometers the range is between 187  
 0.5 and 33 mM.<sup>28</sup> On the basis of these results, the analytical 188  
 reliability of the  $\mu$ PADs treated with nanomaterials was tested 189  
 by performing glucose assay in a clinical sample like human 190  
 urine where the normal concentration levels of glucose are 191  
 between 0.1 and 0.8 mM.<sup>29</sup> For this purpose, an artificial urine 192  
 sample was prepared<sup>5</sup> and spiked with different glucose 193  
 concentration levels to perform the recovery test and therefore 194  
 demonstrate the accuracy of the proposed device. The results 195  
 obtained for artificial urine samples tested with  $\mu$ PADs treated 196  
 with nanomaterial colloid solutions are displayed in Table 1. 197

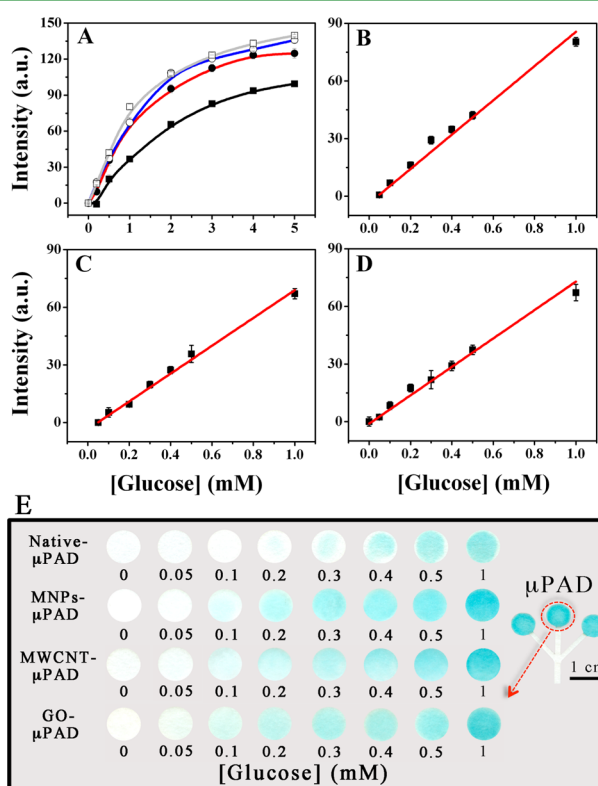


**Figure 4.** (A) Analytical curves for glucose assay using native  $\mu$ PAD (■, black line) and treated  $\mu$ PADs with 100  $\mu$ g mL<sup>-1</sup> of MNPs (□, gray line), 10  $\mu$ g mL<sup>-1</sup> of MWCNT (●, red line), and 100  $\mu$ g mL<sup>-1</sup> of GO (○, blue line). Linear ranges of the analytical curve for glucose using (B) MNPs- $\mu$ PAD, (C) MWCNT- $\mu$ PAD, (D) GO- $\mu$ PAD. (E) Optical images of the detection zones corresponding to glucose assays in concentration ranging from 0–1 mM for native  $\mu$ PAD, MNP- $\mu$ PAD, MWCNT- $\mu$ PAD, and GO- $\mu$ PAD. Error bars displayed in graphs A–D represent the standard deviation value ( $n = 6$ ).

**Table 1. Glucose Concentration Levels Determined on Artificial Urine Samples Using  $\mu$ PADs Treated with Nanomaterials**

known concentration (mM)	found concentration (mM)		
	MNP- $\mu$ PAD	MWCNT- $\mu$ PAD	GO- $\mu$ PAD
0.3	0.16 ± 0.06	0.28 ± 0.08	0.26 ± 0.05
0.4	0.20 ± 0.08	0.37 ± 0.07	0.38 ± 0.04
0.5	0.36 ± 0.11	0.51 ± 0.08	0.56 ± 0.05
0.8	0.61 ± 0.12	0.82 ± 0.08	0.82 ± 0.04

As can be seen in the presented data, we obtained acceptable 198  
 values of glucose concentration determined with MWCNT- 199  
 $\mu$ PADs and GO- $\mu$ PADs in comparison with MNP- $\mu$ PADs. Best 200  
 results were achieved with GO- $\mu$ PADs with recovery values 201  
 between 83 and 109% obtained in a considerable glucose 202  
 concentration range (0.3–0.8 mM) following by MWCNT- 203  
 $\mu$ PADs with recovery values between 76 and 96%. On the other 204  
 hand, the recovery levels for  $\mu$ PADs treated with MNPs were 205  
 between 40 and 71%. This can be related to the presence of 206  
 urea in the artificial urine sample. This compound, as a 207  
 denaturalizing agent, is capable of disrupting enzyme structure 208  
 and therefore decreasing the catalytic activity.<sup>30</sup> On the basis of 209  
 the analytical performance of glucose assay in urine samples, 210

211 the carbon-based nanomaterials used in our study seem to  
212 protect enzymes from urea. Some physical and chemical  
213 characteristics present in carbon-based nanomaterials but not in  
214 MNPs improved the analytical signal for glucose detection in  
215 the tested artificial urine samples.

216 Overall, this study described for the first time the  
217 modification of  $\mu$ PADs by incorporation of MNPs, MWCNT  
218 and GO. The main strategy employed to modify cellulose fibers  
219 with nanomaterials previously synthesized was planned without  
220 the use of any linker, binder or retention aid. The used  
221 procedure solves the drawback of using additives avoiding  
222 possible interaction with enzyme activity. On the basis of the  
223 presented results, the modified  $\mu$ PADs provided enhanced  
224 analytical performance allowing the visual detection of glucose  
225 at low concentrations. The improvements reported in this study  
226 enable the use of proposed devices for POC diagnosis with  
227 many advantages including simple instrumentation, easy  
228 operation, and low cost. Lastly, the association of  $\mu$ PADs  
229 with carbon-based nanomaterials and magnetic nanoparticles  
230 offers great potentiality to be explored in bioanalytical  
231 applications.

## 232 ■ ASSOCIATED CONTENT

### 233 ● Supporting Information

234 The Supporting Information is available free of charge on the  
235 ACS Publications website at DOI: 10.1021/acsami.5b10027.

236 Detailed information on the materials and reagents used,  
237 fabrication of  $\mu$ PADs, and colorimetric detection. Results  
238 of DLS and FT-IR analysis of MNPs, EDS analysis of  
239 MNP- $\mu$ PAD and linear range of the analytical curve of  
240 glucose using native  $\mu$ PADs (PDF)

## 241 ■ AUTHOR INFORMATION

### 242 Corresponding Author

243 \*E-mail: wendell@ufg.br.

### 244 Author Contributions

245 The manuscript was written through contributions of all  
246 authors. All authors have given approval to the final version of  
247 the manuscript.

### 248 Notes

249 The authors declare no competing financial interest.

## 250 ■ ACKNOWLEDGMENTS

251 This project was supported by Conselho Nacional de  
252 Desenvolvimento Científico e Tecnológico (CNPq) (Grants  
253 448089/2014-9 and 311744/2013-3), Fundação de Amparo à  
254 Pesquisa do Estado de Goiás (FAPEG), National Institute of  
255 Science and Technology in Bioanalytics (INCTBio), The  
256 United Nations University Biotechnology Programme for Latin  
257 America and the Caribbean (UNU-BIOLAC) and Consejo  
258 Nacional de Investigaciones Científicas y Técnicas (PIP-  
259 CONICET 112-2011-01-00458). Lastly, the authors thank  
260 Centro Regional para o Desenvolvimento Tecnológico e  
261 Inovação (CRTi) for using their facilities and Dr. Y. Hathcock  
262 for English language revision.

## 263 ■ ABBREVIATIONS

264 TMB, 3,3',5,5'-tetramethylbenzidine  
265 HRP, horseradish peroxidase  
266 GOx, glucose oxidase

## 267 ■ REFERENCES

- (1) Sapsford, K. E.; Algar, W. R.; Berti, L.; Gemmill, K. B.; Casey, B. 268  
J.; Oh, E.; Stewart, M. H.; Medintz, I. L. Functionalizing Nanoparticles 269  
with Biological Molecules: Developing Chemistries that Facilitate 270  
Nanotechnology. *Chem. Rev.* **2013**, *113*, 1904–2074. 271
- (2) Oliveira, O. N., Jr.; Iost, R. M.; Siqueira, J. R., Jr.; Crespilho, F. 272  
N.; Caseli, L. Nanomaterials for Diagnosis: Challenges and 273  
Applications in Smart Devices Based on Molecular Recognition. 274  
*ACS Appl. Mater. Interfaces* **2014**, *6*, 14745–14766. 275
- (3) Scida, K.; Stege, P. W.; Haby, G.; Messina, G. A.; Garcia, C. D. 276  
Recent Applications of Carbon-Based Nanomaterials in Analytical 277  
Chemistry: Critical Review. *Anal. Chim. Acta* **2011**, *691*, 6–17. 278
- (4) Gupta, V. K.; Atar, N.; Yola, M. L.; Eryilmaz, M.; Torul, H.; 279  
Tamer, U.; Boyacı, İ. H.; Üstündağ, Z. A Novel Glucose Biosensor 280  
Platform Based on Ag@AuNPs Modified Graphene Oxide Nano- 281  
composite and SERS Application. *J. Colloid Interface Sci.* **2013**, *406*, 282  
231–237. 283
- (5) Martinez, A. W.; Phillips, S. T.; Butte, M. J.; Whitesides, G. M. 284  
Patterned Paper as a Platform for Inexpensive, Low-Volume, Portable 285  
Bioassays. *Angew. Chem., Int. Ed.* **2007**, *46*, 1318–1320. 286
- (6) Cate, D. M.; Adkins, J. A.; Mettakoonpitak, J.; Henry, C. S. 287  
Recent Developments in Paper-Based Microfluidic Devices. *Anal.* 288  
*Chem.* **2015**, *87*, 19–41. 289
- (7) Ferreira, D. C. M.; Giordano, G. F.; Soares, C. C. S. P.; de 290  
Oliveira, J. F. A.; Mendes, R. K.; Piazzetta, M. H.; Gobbi, A. L.; 291  
Cardoso, M. B. Optical Paper-Based Sensor for Ascorbic Acid 292  
Quantification Using Silver Nanoparticles. *Talanta* **2015**, *141*, 188– 293  
194. 294
- (8) Ornatka, M.; Sharpe, E.; Andreescu, D.; Andreescu, S. Paper 295  
Bioassay Based on Ceria Nanoparticles as Colorimetric Probes. *Anal.* 296  
*Chem.* **2011**, *83*, 4273–4280. 297
- (9) Kumar, A.; Hens, A.; Arun, R. K.; Chatterjee, M.; Mahato, K.; 298  
Layek, K.; Chanda, N. A Paper Based Microfluidic Device for Easy 299  
Detection of Uric Acid Using Positively Charged Gold Nanoparticles. 300  
*Analyst* **2015**, *140*, 1817–1821. 301
- (10) Liang, P.; Yu, H.; Guntupalli, B.; Xiao, Y. Paper-Based Device 302  
for Rapid Visualization of NADH Based on Dissolution of Gold 303  
Nanoparticles. *ACS Appl. Mater. Interfaces* **2015**, *7*, 15023–15030. 304
- (11) Nath, P.; Arun, R. K.; Chanda, N. A Paper Based Microfluidic 305  
Device for the Detection of Arsenic Using a Gold Nanosensor. *RSC* 306  
*Adv.* **2014**, *4*, 59558–59561. 307
- (12) Tsai, T.-T.; Shen, S.-W.; Cheng, C.-M.; Chen, C.-F. Paper-Based 308  
Tuberculosis Diagnostic Devices with Colorimetric Gold Nano- 309  
particles. *Sci. Technol. Adv. Mater.* **2013**, *14*, 044404. 310
- (13) Pourreza, N.; Golmohammadi, H. Application of Curcumin 311  
Nanoparticles in a Lab-On-Paper Device as a Simple and Green pH 312  
Probe. *Talanta* **2015**, *131*, 136–141. 313
- (14) Evans, E.; Gabriel, E. F. M.; Benavidez, T. E.; Coltro, W. K. T.; 314  
Garcia, C. D. Modification of Microfluidic Paper-Based Devices with 315  
Silica Nanoparticles. *Analyst* **2014**, *139*, 5560–5567. 316
- (15) Barsan, M. M.; Ghica, M. E.; Brett, C. M. A. Electrochemical 317  
Sensors and Biosensors Based on Redox Polymer/Carbon Nanotube 318  
Modified Electrodes: a Review. *Anal. Chim. Acta* **2015**, *881*, 1–23. 319
- (16) Tasis, D.; Tagmatarchis, N.; Bianco, A.; Prato, M. Chemistry of 320  
Carbon Nanotubes. *Chem. Rev.* **2006**, *106*, 1105–1136. 321
- (17) Feng, W.; Ji, P. Enzymes Immobilized on Carbon Nanotubes. 322  
*Biotechnol. Adv.* **2011**, *29*, 889–895. 323
- (18) Shemetov, A. A.; Nabiev, I.; Sukhanova, A. Molecular 324  
Interaction of Proteins and Peptides with Nanoparticles. *ACS Nano* 325  
**2012**, *6*, 4585–4602. 326
- (19) Zhang, J.; Zhang, F.; Yang, H.; Huang, X.; Liu, H.; Zhang, J.; 327  
Guo, S. Graphene Oxide as a Matrix for Enzyme Immobilization. 328  
*Langmuir* **2010**, *26*, 6083–6085. 329
- (20) Rossi, L. M.; Quach, A. D.; Rosenzweig, Z. Glucose Oxidase– 330  
Magnetite Nanoparticle Bioconjugate for Glucose Sensing. *Anal.* 331  
*Bioanal. Chem.* **2004**, *380*, 606–613. 332
- (21) Khoshnevisan, K.; Bordbar, A. K.; Zare, D.; Davoodi, D.; 333  
Noruzi, M.; Barkhi, M.; Tabatabaei, M. Immobilization of Cellulase 334

- 335 Enzyme on Superparamagnetic Nanoparticles and Determination of its  
336 Activity and Stability. *Chem. Eng. J.* **2011**, *171*, 669–673.
- 337 (22) Dong, Y. L.; Zhang, H. G.; Rahman, Z. U.; Su, L.; Chen, X. J.;  
338 Hu, J.; Chen, X. G. Graphene Oxide–Fe<sub>3</sub>O<sub>4</sub>Magnetic Nano-  
339 composites with Peroxidase-Like Activity for Colorimetric Detection  
340 of Glucose. *Nanoscale* **2012**, *4*, 3969–3976.
- 341 (23) Wei, H.; Wang, E. Fe<sub>3</sub>O<sub>4</sub>Magnetic Nanoparticles as Peroxidase  
342 Mimetics and Their Applications in H<sub>2</sub>O<sub>2</sub> and Glucose Detection.  
343 *Anal. Chem.* **2008**, *80*, 2250–2254.
- 344 (24) Henstridge, M. C.; Compton, R. G. Mass Transport to Micro  
345 and Nanoelectrodes and Their Arrays: A Review. *Chem. Rec.* **2012**, *12*,  
346 63–71.
- 347 (25) Laurent, S.; Forge, D.; Port, M.; Roch, A.; Robic, C.; Vander  
348 Elst, L.; Muller, R. N. Magnetic Iron Oxide Nanoparticles: Synthesis,  
349 Stabilization, Vectorization, Physicochemical Characterizations, and  
350 Biological Applications. *Chem. Rev.* **2008**, *108*, 2064–2110.
- 351 (26) Qi, H.; Liu, J.; Mäder, E. Smart Cellulose Fibers Coated With  
352 Carbon Nanotube Networks. *Fibers* **2014**, *2*, 295–307.
- 353 (27) Chauhan, I.; Aggrawal, S.; Mohanty, C.; Mohanty, P. Metal  
354 Oxides Nanostructures Incorporated/Immobilized Paper Matrices and  
355 Their Applications: A Review. *RSC Adv.* **2015**, *5*, 83036–83055.
- 356 (28) Bahadir, E. B.; Sezgintürk, M. K. Applications of Commercial  
357 Biosensors in Clinical, Food, Environmental and Biothreat/Bio warfare  
358 Analyses. *Anal. Biochem.* **2015**, *478*, 107–120.
- 359 (29) McPherson, R. A.; Pincus, M. R. *Henry's Clinical Diagnosis and*  
360 *Management by Laboratory Methods*, 22nd ed; Elsevier Saunders:  
361 Philadelphia, 2011.
- 362 (30) Rauf, S.; Ihsan, A.; Akhtar, K.; Ghauri, M. A.; Rahman, M.;  
363 Anwar, M. A.; Khalid, A. M. Glucose Oxidase Immobilization on a  
364 Novel Cellulose Acetate–Polymethylmethacrylate Membrane. *J.*  
365 *Biotechnol.* **2006**, *121*, 351–360.